ELSEVIER

Thermochimica Acta 267 (1995) 195–208

thermochimica acta

A kinetic study of the thermal decomposition of iron(III) hydroxide-oxides 2. Preparation and thermal decomposition of γ-FeO(OH)[1]

Nobuyoshi Koga[a,*], Shougo Okada[a], Tatsuya Nakamura[b], Haruhiko Tanaka[a]

[a]*Chemistry Laboratory, Faculty of School Education, Hiroshima University, 3-1-33 Shinonome, Minami-ku, Hiroshima 734, Japan*

[b]*Research and Development Division, Toda Kogyo Corporation, 4-1-2 Funairi-minami, Hiroshima 730, Japan*

Received 30 January 1995; accepted 4 May 1995

Abstract

Hydrated and anhydrous γ-FeO(OM) with different sizes and shapes of crystalline powders were prepared through an oxidative hydrolysis of iron(II) chloride solution using urea decomposition. Systematic thermogravimetric measurements under isothermal and non-isothermal conditions were performed in order to characterize kinetically the thermal dehydration and dehydroxylation processes. The dehydration of the bound water on the surface of γ-FeO(OH) observed at around 150°C obeyed the first-order law with an apparent activation energy of about 100 kJ mol^{-1}, being recognized as controlled by diffusional removal of evolved water vapor through the stacking assemblage of plate-like crystalline powders. As for the hydrated γ-FeO(OH), the thermal dehydroxylation process at around 280°C, subsequent to thermal dehydration of the bound water, was well characterized by the two-dimensional phase boundary controlled reaction law R_2 with apparent activation energy of about 150 kJ mol^{-1}, implying shrinkage of the reaction interface from the edge of the rectangular plate. The Avrami-Erofeyev A_m law was estimated for the dehydroxylation process of the anhydrous samples, in which the kinetic exponents m in the A_m law increased with increasing specific surface area and the aspect ratio of the rectangular plate of the sample powders.

Keywords: Hydrated γ-FeO(OH); Anhydrous γ-FeO(OH); Kinetics; Thermal dehydration; Thermal dehydroxylation; TG-DTG

* Corresponding author.

[1] Presented at the 30th Anniversary Conference of the Japan Society of Calorimetry and Thermal Analysis, Osaka, Japan, 31 October–2 November 1994.

SSDI 0040-6031 (95) 02478-6

1. Introduction

It is well known that the kinetics of thermal decomposition of solids depends largely on the sample and reaction conditions [1–3]. The morphology and physico-chemical properties of the product solid are thus affected by both the applied conditions and the kinetics of the thermal decomposition. Accordingly, systematic understanding of the decomposition kinetics is required to control the properties of the decomposition product. In the present series of kinetic studies on the thermal decomposition of iron(III) hydroxide oxides [4], we attempted to evaluate the relationships of the decomposition kinetics with the morphology, the particle size and distribution of the sample, which are controlled in preparation. Because the thermal decomposition of iron(III) salts is one of the most important processes in preparing iron(III) oxides, a systematic understanding of the kinetics is expected to result in some useful findings for controlling the properties of the solid product.

It has been reported [5,6] that excess water molecules hydrated to γ-FeO(OH) can be characterized as "bound" water on the surface of the original γ-FeO(OH) and dehydration of the bound water takes place at around 150°C. Anhydrous γ-FeO(OH) decomposes to less crystalline γ-Fe_2O_3, followed by exthothermic phase transformation and/or crystallization to α-Fe_2O_3 at around 400°C [7]. In this work, both hydrated and anhydrous γ-FeO(OH) were prepared through oxidative hydrolysis of iron(II) chloride solutions using urea decomposition. The morphology of the sample particle was controlled by changing the period of suspending the precipitate in the mother solution. The systematic kinetic analyses of thermogravimetric (TG) curves for the thermal dehydration and/or decomposition under isothermal and non-isothermal conditions were performed employing the methods of kinetic analysis described earlier [4,8–10]. The relationship between the transformation kinetics and the morphology of the reactant solids is discussed on the basis of the kinetic parameters calculated in the present study.

2. Experimental

2.1. Sample preparation

Reagent grade $FeCl_2 \cdot nH_2O$ (Katayama Chem. Ind. Co.) (15 g) was dissolved in distilled water to prepare 800 ml of dilute solution. Reagent grade urea (Katayama Chem. Ind. Co.) (60 g) was dissolved in the solution. The solution was stirred mechanically at 50°C for different periods: 7, 15, 21, and 30 days. Oxygen dissolved in the atmosphere led to oxidation of Fe^{2+} to Fe^{3+} and hydrolytic precipitation of ferric hydroxide-oxide. After filtering and washing with distilled water until chloric ions were no longer detected in the filtrate, the precipitates were dried at 70°C for 5 h. The precipitates prepared by digesting for 7, 15, 21 and 30 days were designated as samples (a), (b), (c), and (d), respectively.

2.2. Characterization

Powder X-ray diffraction (XRD) measurements were carried out using a Rigaku

miniflex diffractometer (Mn filtered Fe-Ka, 30 kV, 10 mA) in order to identify the precipitated phase. XRD patterns of the sample heated at various constant temperatures in an electric furnace for 10 h were also obtained. FT-IR spectra of the precipitates were obtained using a Shimadzu FT-IR8100 spectrophotometer by the diffuse reflectance method. The specific surface area of the precipitates was measured using the BET method. The particle size and shape of the precipitates were observed with transmission electron microscopy (JEOL, JEM-100S, acceleration voltage 100 kV) after pouring an aqueous suspension of the sample powder onto a carbon mesh on a copper grid. Simultaneous measurements of TG-DTA were carried out using ULVAC TGD-9400 apparatus at a heating rate of 10 K min^{-1} in flowing N_2 at a rate of 50 ml min^{-1}. α-Al_2O_3 was used as the reference material for the DTA measurements.

2.3. Kinetic measurement

Systematic TG measurements were done on a Shimadzu TGA50 in order to characterize kinetically the thermal decomposition processes of the precipitates. Samples of 5.0 mg were weighed onto a platinum crucible, 5 mm in diameter and 2.5 mm in height. Isothermal mass-loss traces were obtained at various constant temperatures in flowing N_2 at a rate of 30 ml min^{-1}. Non-isothermal TG-DTG measurements were also carried out at various heating rates ranging from 0.5 to 8.0 K min^{-1} under the conditions otherwise identical with those for the isothermal runs.

3. Results and discussion

Fig. 1 shows the change in pH values of the solution with stirring at 50°C. During the

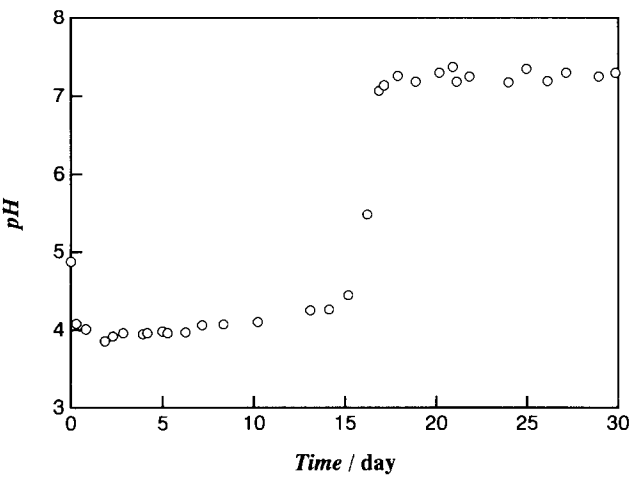

Fig. 1. Change in the pH value during the preparation of γ-FeO(OH) through oxidative hydrolysis of an iron(II) chloride solution using urea decomposition.

precipitation reaction, the pH was maintained at around 4.0. After completing the precipitation reaction, the pH of the solution rose to about 7.0 by decomposing urea. The precipitates obtained after stirring the reactant solution for 7, 15, 21 and 30 days were subjected to further physico-chemical investigations.

Figs. 2 and 3 represent typical XRD patterns and FT-IR spectra of the precipitates, respectively. Nominally the same XRD and FT-IR patterns were obtained for the precipitates irrespective of the periods of stirring. Diffraction peaks in Fig. 2 correspond to those of γ-FeO(OH), except the small diffraction peak, corresponding to α-FeO(OM), observed at 26.30 for sample (a) The diffraction peak due to α-FeO(OM) disappears for the samples obtained by stirring the suspension longer than 7 days. The IR absorption peaks at 2890, 1020 and 747 cm^{-1} are characteristic of γ-FeO(OH), being due to O–H stretching, O–H bending and Fe–O stretching vibrations, respectively [11]. The major difference in the IR patterns among the samples is seen for sample (b) within the range of 1400–1700 cm^{-1}. Fig. 4 shows TEM photographs of the respective samples. Plate like rectangular crystals are seen with different crystal sizes depending on the period of digestion. The specific surface areas of the respective samples determined from the BET method are shown in Fig. 5, together with the mean aspect ratio on the rectangular face measured from the TEM photographs. It can be seen from Fig. 5 that the crystal size is maximum at the final stage of the precipitation reaction, followed by a decrease in the crystalline size through the ageing at pH 7.0. This might be due to dissolution, since γ-FeO(OH) is stable only in acidic media. The change in the specific surface area is accompanied by change

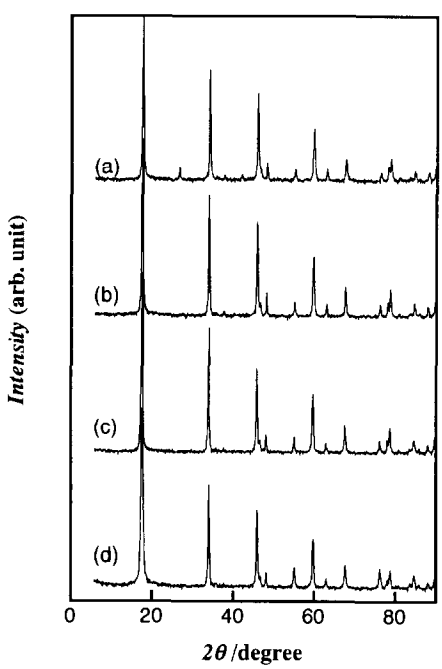

Fig. 2. The XRD patterns for samples (a) 7, (b) 15, (c) 21, and (d) 30 days.

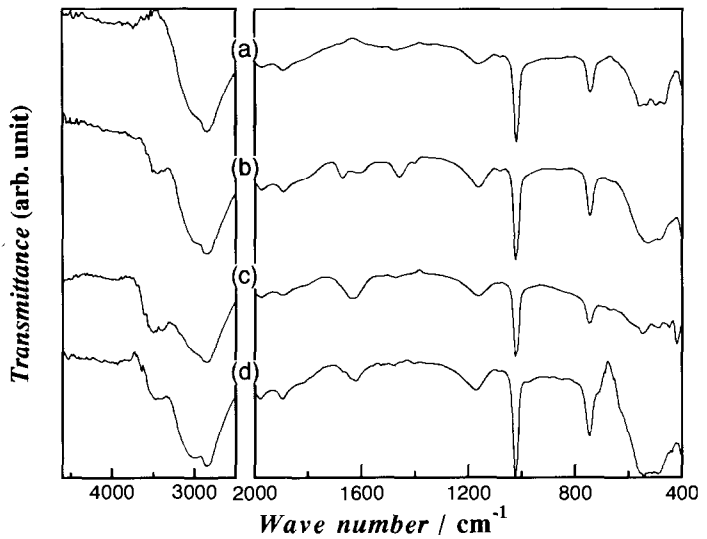

Fig. 3. The FT-IR spectra for samples (a) 7, (b) 15, (c) 21, and (d) 30 days.

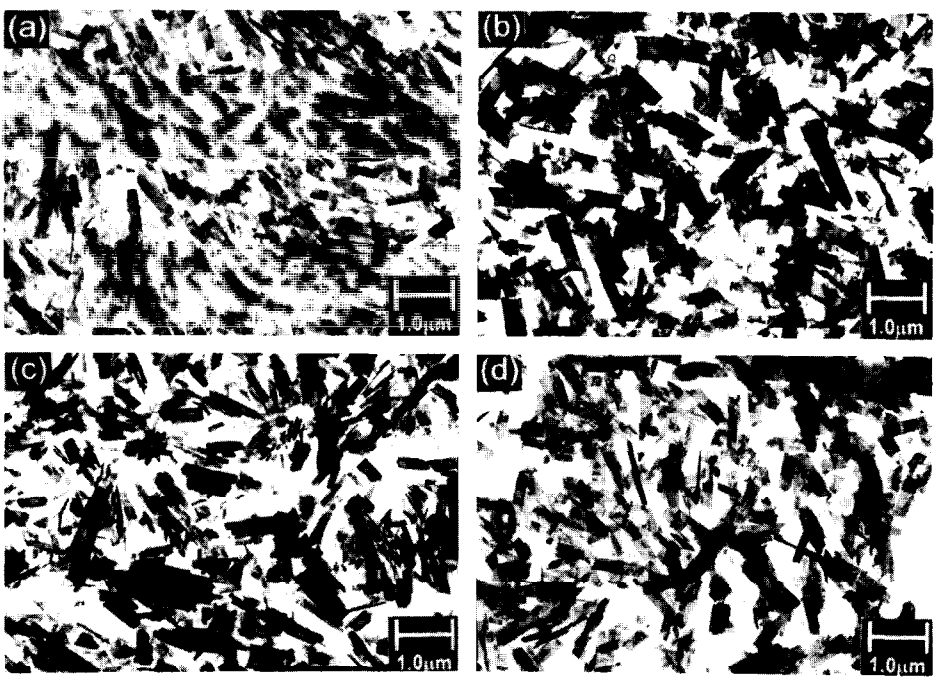

Fig. 4. The TEM photographs for samples (a) 7, (b) 15, (c) 21, and (d) 30 days.

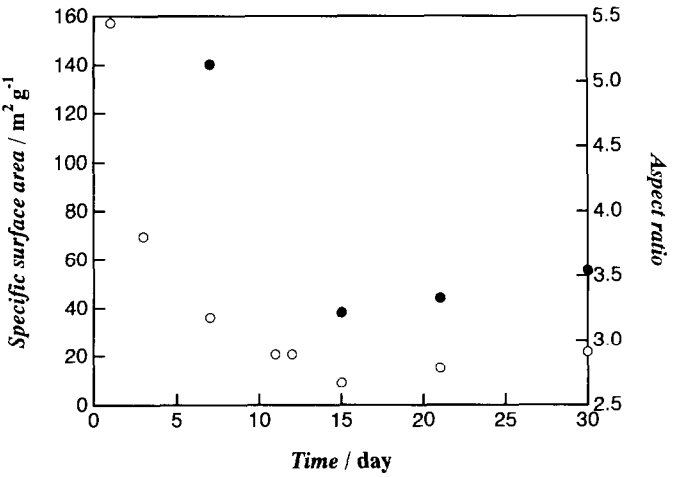

Fig. 5. Changes in the specific surface area and aspect ratio of the rectangular plate of the crystalline powder digested in the mother solution.

in the aspect ratio, indicating that crystal growth takes place to reduce the aspect ratio of the rectangle. TG-DTA curves of the respective samples are shown in Fig. 6. Although the adsorbed water was released at temperatures lower than 100°C, mass loss due to thermal decomposition of the samples at around 280°C observed for samples (a), (c), and (d) corresponds quantitatively to the thermal decomposition of FeO(OH) to Fe_2O_3. Sam-

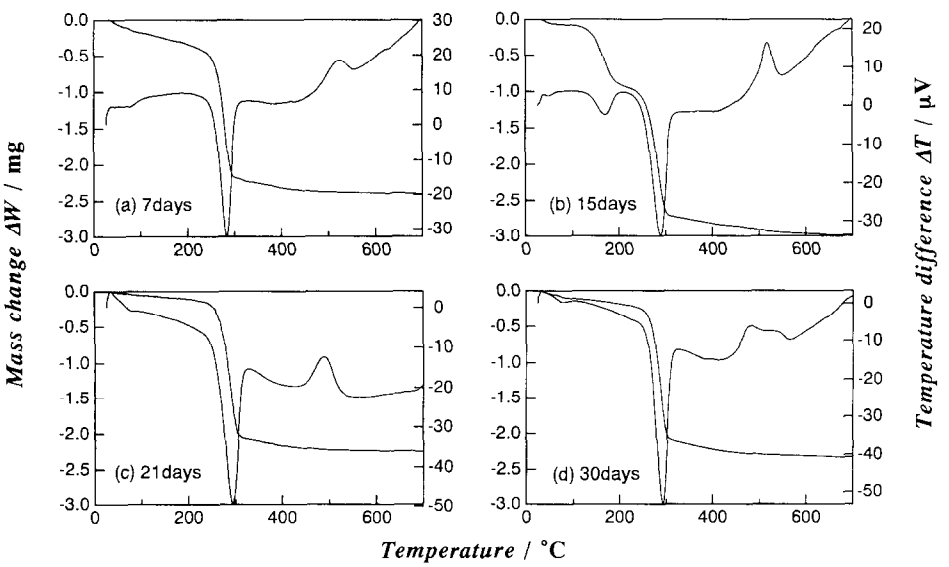

Fig. 6. Simultaneous TG-DTA curves obtained at a heating rate of 10 K min^{-1} using 30.0 mg samples (a) 7, (b) 15, (c) 21, and (d) 30 days.

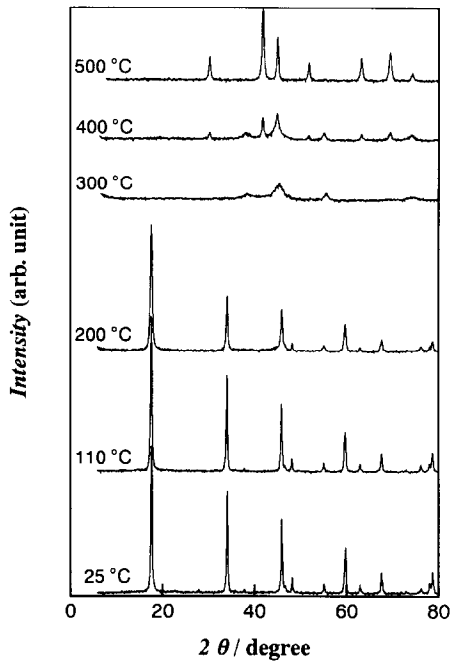

Fig. 7. Typical XRD patterns for hydrated γ-FeO(OH). Sample (b) 15 days, heated at various temperatures in a static atmosphere of air.

ple (b) represents a different decomposition behavior of the two steps, characterized as the thermal dehydration of bound water and dehydroxylation, respectively. Considering the mass loss in the TG curves, the hydrated γ-FeO(OH) is expressed as $FeO(OH)\cdot 0.2H_2O$. Such hydrated γ-FeO(OH) was obtained during the course of the variation of pH from 4.0 to 7.0. The different IR absorption behavior observed for sample (b) within the range of 1400–1700 cm^{-1} is likely due to the existence of the bound water.

3.1. Thermal dehydration of hydrated γ-FeO(OH)

Fig. 7 shows the XRD patterns of sample (b) heated at various temperatures. Comparing the XRD patterns at 110 and 200°C, it is seen that no change is observed in the temperature region corresponding to the first mass loss process, indicating the thermal dehydration of bound water. On heating the sample at 300°C, the XRD shows the change from the pattern of orthorhombic γ-FeO(OH) to that of inverse spinel cubic γ-Fe_2O_3. From the XRD patterns obtained after heating the sample at 300, 400, and 500°C, it is seen that the exothermic DTA peak observed at around 500°C (see Fig. 6b), corresponds to the transformation of the orthorhombic γ-Fe_2O_3 to rhombohedral α-Fe_2O_3 [12].

Fig. 8 shows typical plots of the fractional reaction α against time t for isothermal dehydration at various temperatures. Agreement of data to the appropriate kinetic rate

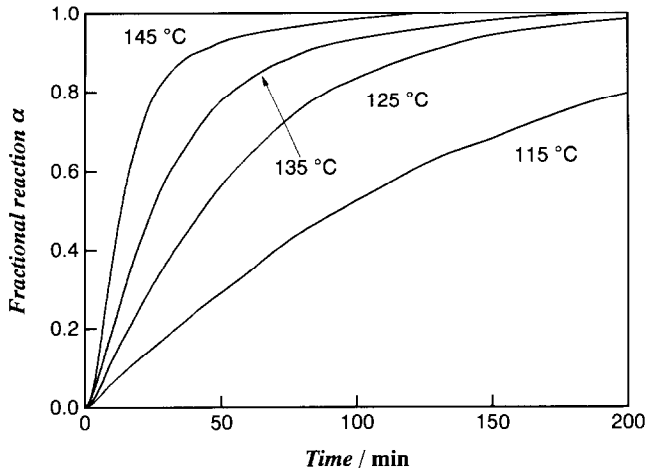

Fig. 8. Typical α versus t plots for the isothermal dehydration of hydrated γ-FeO(OH) sample (b) 15 days, at various constant temperatures.

equation, $g(\alpha) = kt$, was compared through plots of all possible $g(\alpha)$, listed elsewhere [1–3], against t. The fairly linear plots were obtained in terms of the first order F_1 law, $-\ln(1-\alpha) = kt$, irrespective of the temperatures examined. The F_1 law is also recognized as an Avrami-Erofeyev A_m law, $[-\ln(1-\alpha)]^{1/m} = kt$ with $m = 1$, formulated by assuming one-dimensional growth of pre-existing nuclei. Table 1 lists the values of k obtained from the slope of $-\ln(1-\alpha)$ against t plots at various temperatures, together with the apparent activation energy E and logarithmic preexponential factor A calculated from the Arrhenius plots.

Fig. 9 shows kinetic rate data obtained from non-isothermal TG-DTG curves for the thermal dehydration, as plots of α against the temperature T. For analyzing the non-

Table 1

Apparent values of k for isothermal dehydration of hydrated γ-FeO(OH) at various temperatures, together with the Arrhenius parameters calculated

Temperature/°C	$k \times 10^4$	γ^a
115	1.25	0.9997
125	2.91	0.9999
130	4.54	0.9998
140	7.95	0.9994
150	17.6	0.9996
E/k mol^{-1}	103 ± 4	
log A/s^{-1}	9.98 ± 0.52	
$-\gamma^b$	0.9974	

[a] Correlation coefficient of the linear regression analysis of the $g(\alpha)$ vs. t plot.
[b] Correlation coefficient of the linear regression analysis of the Arrhenius plot.

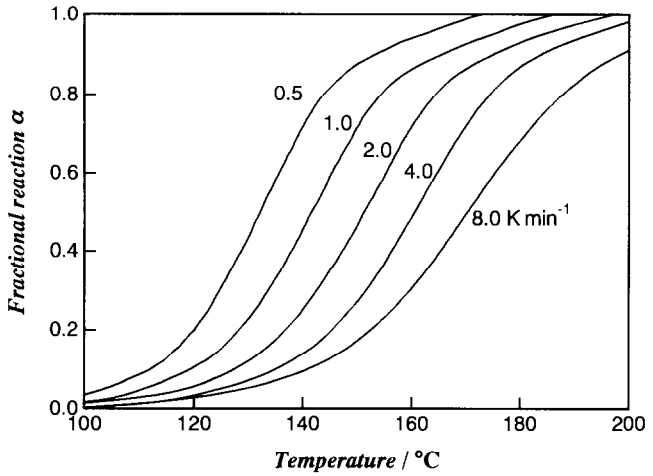

Fig. 9. Typical α versus T plots for non-isothermal dehydration of hydrated γ-FeO(OH) sample (b) 15 days, at various heating rates.

isothermal kinetics, a differential isoconversion method of the extended Friedman [13,14] was employed assuming the logarithmic form of the general kinetic equation:

$$\ln\left(\frac{d\alpha}{dt}\right) = \ln[Af(\alpha)] - \frac{E}{RT} \tag{1}$$

where $f(\alpha)$ is the kinetic model function in differential form. By plotting $\ln(d\alpha/dt)$ against $1/T$, the apparent values of E at different α were obtained from the slope. The constant value of $E = 108 \pm 3$ kJ mol^{-1} was obtained within the restricted range of $0.2 \leq \alpha \leq 0.8$, which is one of the prerequisites for the further kinetic characterization in terms of the general kinetic equation [15]. Introducing the generalized time θ [16,17], the rate data were extrapolated to the infinite temperature according to the equation:

$$\frac{d\alpha}{d\theta} = \frac{d\alpha}{dt}\exp\left(\frac{E}{RT}\right) = Af(\alpha) \tag{2}$$

where $d\alpha/d\theta$ indicates the transformation rate at infinite temperature. Fig. 10 shows the kinetic rate data at infinite temperature as a plot of $d\alpha/d\theta$ against α. The value of $d\alpha/d\theta$ decreases monotonously with α, indicating possible obedience to the F_1 law as is the case with isothermal dehydration. The apparent preexponential factor obtained from the slope of $d\alpha/d\theta$ versus $-\ln(1-\alpha)$ was $A = 3.5 \times 10^{10}$ s^{-1}. The Arrhenius parameters determined for the non-isothermal dehydration are in good agreement with those of isothermal dehydration.

Taking into account the properties of the bound water on the surface of the γ-FeO(OH) crystals, kinetic obedience to the F_1 law seems to imply diffusional removal

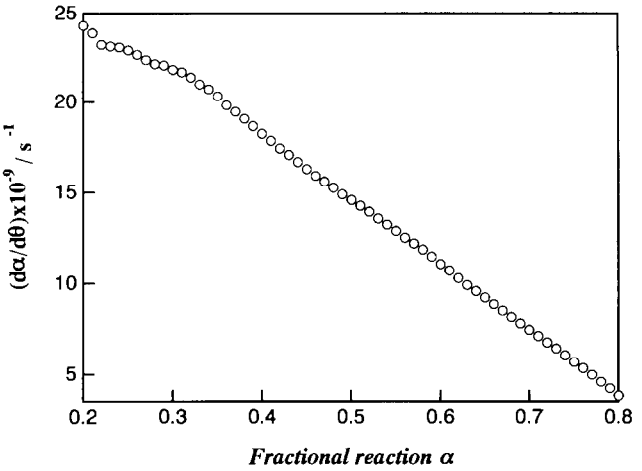

Fig. 10. A plots of $d\alpha/d\theta$ against α for non-isothermal dehydration of hydrated γ-FeO(OH), sample (b) 15 days.

of water vapor through the stacking assemblage of the plate-like crystals [18], rather than one-dimensional growth of pre-exiting nuclei assumed in formulating the A_1 law [1].

3.2. Thermal dehydroxylation of γ-FeO(OH)

Fig. 11 represents a comparison of the isothermal kinetic rate data for thermal dehy-

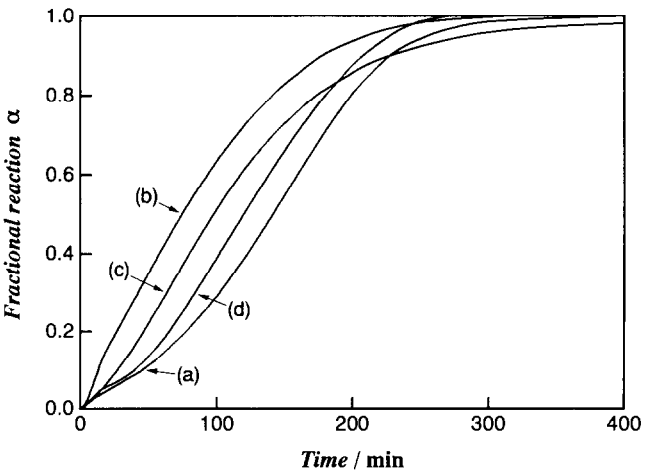

Fig. 11. Typical α versus t plots for isothermal dehydroxylation of γ-FeO(OH) at 220°C for samples (a) 7, (b) 15, (c) 21, and (d) 30 days.

Table 2

The kinetic parameters obtained for the isothermal dehydroxylation of γ-FeO(OH)

Sample	(a) 7 days		(b) 15 days		(c) 21 days		(d) 30 days	
$g(\alpha)$	A_m ($m = 4.0$)		R_n ($n = 2.1$)		A_m ($m = 1.5$)		A_m ($m = 2.8$)	
Temp./°C	$k \times 10^4/s^{-1}$	γ^a	$k \times 10^4/s^{-1}$	γ^a	$k \times 10^4/s^{-1}$	γ^a	$k \times 10^4/s^{-1}$	γ^a
210	0.301	0.9999	0.269	0.9998	0.598	0.9999	0.414	0.9994
215	0.408	0.9999	0.387	0.9996	0.801	0.9998	–	–
290	0.607	0.9999	0.628	0.9999	1.29	0.9996	0.879	0.9997
930	1.37	0.9998	1.22	0.9998	2.64	0.9999	1.81	0.9998
940	–	–	2.39	0.9999	5.55	0.9998	3.73	0.9996
950	3.79	0.9987	–	–	1.00	0.9997	6.09	0.9998
E/kJ mol^{-1}	144 ± 5		155 ± 5		155 ± 4		147 ± 5	
log A/s^{-1}	11.1 ± 0.5		12.2 ± 0.5		12.6 ± 0.4		11.5 ± 0.5	
$-\gamma^b$	0.9986		0.9991		0.9996		0.9983	

[a] Correlation coefficient of the linear regression analysis of the $g(\alpha)$ versus t plot.

[b] Correlation coefficient of the linear regression analysis of the Arrhenius plot.

droxylation measured at a programmed temperature of 220°C. The kinetic curves for samples (a) and (d) are sigmoidal. The induction period decreases in samples (b) and (c). Different kinetic behavior among the samples is expected from the shape of the respective kinetic curves. Through the plots of possible $g(\alpha)$ against t, the A_m law was estimated for the dehydroxylation process of samples (a), (c) and (d). The dehydroxylation of sample (b) satisfactorily obeyed the phase boundary controlled R_n law, $1-(1-\alpha)=kt$. The most appropriate $g(\alpha)$, which represents the best linearity of the $g(\alpha)$ versus t plots, was obtained by changing the values of kinetic exponent m and n in the A_m and R_n laws, respectively. Table 2 lists the $g(\alpha)$ selected and the apparent values of k at various temperatures, together with the Arrhenius parameters calculated. The kinetic exponent m in the A_m law was larger for the sample with larger specific surface area and aspect ratio of the rectangular plate. Approximately identical values of the Arrhenius parameters were obtained irrespective of the samples.

The non-isothermal kinetic curves for thermal dehydroxylation of respective samples at a programmed heating rate of 4.0 K min^{-1} are shown in Fig. 12. With increasing specific surface area (see Fig. 1), the decomposition temperature shifts to a higher temperature region and the maximum reaction rate increases. Fig. 13 shows the α dependence of the apparent values of F calculated by the Friedman method. The nearly constant values of F for the respective samples were obtained in the restricted range of $0.2 \leq \alpha \leq 0.8$. Table 3 lists the mean value of F in the range of $0.2 \leq \alpha \leq 0.8$. A slightly larger value of F was obtained for sample (b), being different from the case of the isothermal dehydroxylation (see Table 2). Fig. 14 shows the comparison of the shapes of $d\alpha/d\theta$ against α plots. The α value at maximum $d\alpha/d\theta$ shifts to larger α with increasing specific surface area. The kinetic obedience of the non-isothermal dehydroxylation process was determined by plotting the possible $f(\alpha)$ against $d\alpha/d\theta$ (see Eq. (2)). As is the case with isothermal dehydroxylation, samples (a), (c) and (d) obeyed the A_m law and the process for

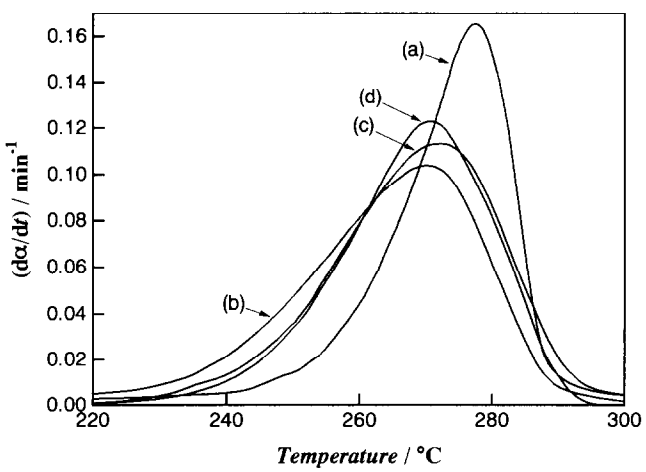

Fig. 12. Typical $d\alpha/dt$ versus T plots for non-isothermal dehydroxylation of γ-FeO(OH) at a heating rate of 4 K min^{-1} for samples (a) 7, (b) 15, (c) 21, and (d) 30 days.

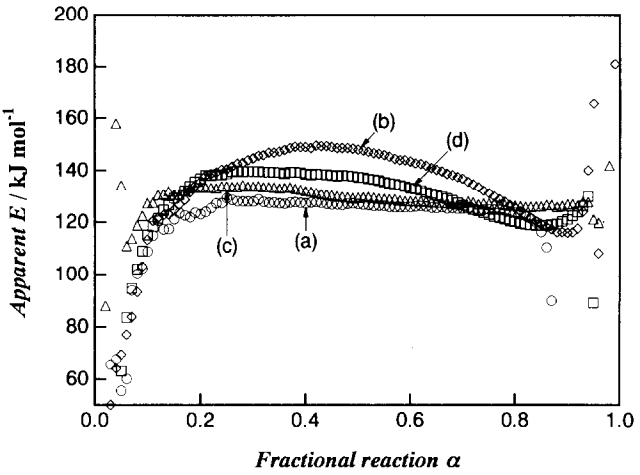

Fig. 13. Apparent values of E at various α for non-isothermal dehydroxylation of γ-FeO(OH) for samples (a) 7, (b) 15, (c) 21, and (d) 30 days.

sample (b) was satisfactorily characterized by the R_n laws. Table 3 also lists the most appropriate $f(\alpha)$ giving the best linearity of the $d\alpha/d\theta$ versus $f(\alpha)$ plots, together with the value of A calculated from the slope of the $d\alpha/d\theta$ versus $f(\alpha)$ plots.

Kinetic obedience to the R_2 law was estimated for the thermal dehydroxylation process of sample (b) under both isothermal and non-isothermal conditions. The Arrhenius parameters also show fairly good agreement between the isothermal and non-isothermal dehydroxylations. It is expected for sample (b) that the reaction proceeds geometrically according to the advancement of the reaction interface from the edge of the rectangular plate. Samples (a), (c) and (d) decompose according to the A_m law, in which the kinetic exponent m decreases with decreasing specific surface area and aspect ratio of the rectangular plate. Slightly smaller values of m and the Arrhenius parameters were obtained for the non-isothermal dehydroxylation, being likely due to the change in the nucleation behavior of the product crystallites between the isothermal and non-isothermal conditions. The kinetic behavior of the dehydroxylation process is apparently influenced by the existence of bound water on the surface of γ-FeO(OH).

Table 3

The kinetic parameters obtained for the non-isothermal dehydroxylation of γ-FeO(OH)

Sample	E/kJ mol^{-1}	$f(\alpha)$	A/s^{-1}	γ^a
(a) 7 days	130 ± 2	$A_{3.1}$	3.96×10^9	0.9888
(b) 15 days	142 ± 4	$R_{1.9}$	1.05×10^9	0.9991
(c) 21 days	130 ± 2	$A_{1.5}$	1.09×10^{10}	0.9996
(d) 30 days	134 ± 4	$A_{1.9}$	2.36×10^{10}	0.9980

[a] Correlation coefficient of the linear regression analysis of the $d\alpha/d\theta$ vs. $f(\alpha)$ plot.

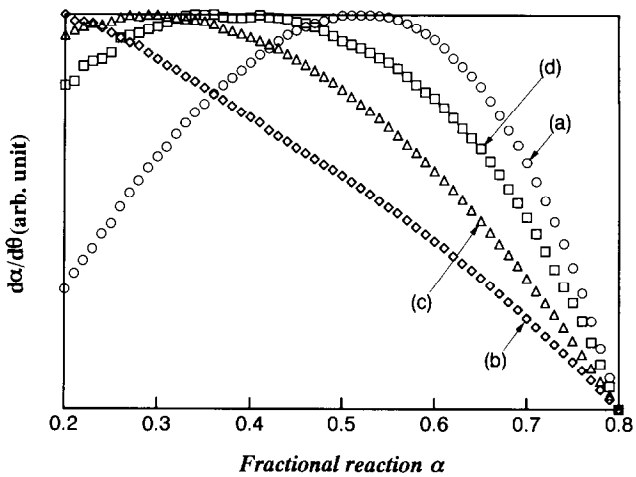

Fig. 14. Comparison of the $d\alpha/d\theta$ versus α plots for non-isothermal dehydroxylation of γ-FeO(OH) for samples (a) 7, (b) 156, (c) 21, and (d) 30 days.

Different properties of the product γ-Fe_2O_3 affected by the sample characteristics and dehydroxylation kinetics are expected from the different transition behavior of the dehydroxylation product to α-Fe_2O_3 detected from corresponding DTA exothotherms (see Fig. 6). A DSC study of the transformation kinetics is in progress to evaluate the effect of the dehydroxylation kinetics on the following phase transition kinetics, together with morphological characterization of the dehydroxylation product γ-Fe_2O_3.

References

[1] M.E. Brown, D. Dollimore and A.K. Galwey, Reactions in the Solid State, Elsevier, Amsterdam, 1980.
[2] J. Sestak, Thermophysical Properties of Solids, Elsevier, Amsterdam, 1984.
[3] O.F. Shlensky, L.N. Aksenov and A.G. Shashkov, Thermal Decomposition of Materials, Elsevier, Amsterdam, 1991.
[4] N. Koga, S. Takemoto, S. Okada and H. Tanaka, Thermochim. Acta, in press.
[5] G. Okamoto, R. Furuichi and N. Sato, Electrochim. Acta, 12 (1967) 1287.
[6] T. Ishikawa, S. Nitta and S. Kondo, J. Chem. Soc., Faraday Trans., 82 (1986) 2401.
[7] T. Ishikawa and K. Inouye, Bull. Chem. Soc. Jpn., 45 (1972) 2350.
[8] N. Koga, J. Malek, J. Sestak and H. Tanaka, Netsu Sokutei (Calor. Therm. Anal.), 20 (1993) 210.
[9] N. Koga and H. Tanaka, Thermochim. Acta, 240 (1994) 141.
[10] N. Koga and H. Tanaka, J. Phys. Chem., 98 (1994) 10521.
[11] K. Inouye, Kagaku to Kogyo, 27 (1974) 571 (in Japanese).
[12] W. Lodding and L. Hammel, Anal. Chem., 32 (1960) 657.
[13] H.L. Friedman, J. Polym. Sci., C6 (1964) 183.
[14] T. Ozawa, J. Therm. Anal., 31 (1986) 547.
[15] N Koga, Thermochim. Acta, 244 (1994) 1.
[16] T. Ozawa, Bull. Chem. Soc. Jpn., 38 (1965) 1881.
[17] T. Ozawa, Thermochim. Acta, 100 (1986) 109.
[18] V.B Okhotnikov, React. Kinet. Catal. Lett., 38 (1989) 359.